

Oxygen Activation and Arene Hydroxylation by Functional Mimics of α -Keto Acid-Dependent Iron(II) Dioxygenases

Eric L. Hegg, Raymond Y. N. Ho, and Lawrence Que, Jr.*

Department of Chemistry and Center for Metals in Biocatalysis
University of Minnesota, Minneapolis, Minnesota 55455

Received November 9, 1998

α -Keto acid-dependent enzymes, which represent the largest and most diverse class of non-heme iron enzymes, utilize an α -keto acid cofactor to effect dioxygen activation in numerous biochemical pathways (Scheme 1).^{1,2} Crystallographic studies of one member of this class, deacetoxycephalosporin C synthase (DAOCS),³ reveal a 2-His-1-carboxylate facial triad at the iron center, an emerging motif among mononuclear nonheme iron enzymes.⁴ In the enzyme-cofactor complex, the α -ketoglutarate (α -KG) cofactor is chelated to the iron through the carboxylate and the α -keto oxygen. These crystal structures confirm the model previously proposed based on various spectroscopic and biochemical studies.^{2,5} While the few model iron(II)– α -keto acid complexes available^{6,7} have provided important mechanistic insight, they have not demonstrated the dioxygenase reactivity exhibited by the enzymes. Here we report the structure and properties of $[\text{Fe}(\text{Tp}^{\text{Ph}_2})(\text{BF})]$ (**1**),⁸ which reacts with O_2 to effect intramolecular arene hydroxylation, incorporating both atoms of O_2 into the products and thus demonstrating for the first time the dioxygenase activity exhibited by α -keto acid-dependent enzymes. In addition, the reactivity of **1** is contrasted with that of $[\text{Fe}(\text{Tp}^{\text{Ph}_2})(\text{OBz})]$, emphasizing the unique function of the α -keto acid cofactor in oxygen activation.

(1) Abbott, M. T.; Udenfriend, S. In *Molecular Mechanisms of Oxygen Activation*; Hayaishi, O., Ed.; Academic Press: New York, 1974; pp 167–214.

(2) Que, L., Jr.; Ho, R. Y. N. *Chem. Rev.* **1996**, *96*, 2607–2624.

(3) Valegard, K.; van Scheltinga, A. C. T.; Lloyd, M. D.; Hara, T.; Ramaswamy, S.; Perrakis, A.; Thompson, A.; Lee, H.-J.; Baldwin, J. E.; Schofield, C. J.; Hajdu, J.; Andersson, I. *Nature* **1998**, *394*, 805–809.

(4) Hegg, E. L.; Que, L., Jr. *Eur. J. Biochem.* **1997**, *250*, 625–629.

(5) Pavel, E. G.; Zhou, J.; Busby, R. W.; Gunsior, M.; Townsend, C. A.; Solomon, E. I. *J. Am. Chem. Soc.* **1998**, *120*, 743–753.

(6) Chiou, Y.-M.; Que, L., Jr. *J. Am. Chem. Soc.* **1995**, *117*, 3999–4013.

(7) Ha, E. H.; Ho, R. Y. N.; Kisiel, J. F.; Valentine, J. S. *Inorg. Chem.* **1995**, *34*, 2265–2266.

(8) Abbreviations: BF, benzoylformate; DAOCS, deacetoxycephalosporin C synthase; α -KG, α -ketoglutarate; MLCT, metal-to-ligand charge transfer; $\text{Tp}^{\text{Bu}_i\text{-Pr}}$, hydrotris(3-*tert*-butyl-5-isopropylpyrazol-1-yl)borate; Tp^{Me_2} , hydrotris(3,5-dimethylpyrazol-1-yl)borate; Tp^{Ph_2} , hydrotris(3,5-diphenylpyrazol-1-yl)borate.

(9) Kitajima, N.; Fujisawa, K.; Fujimoto, C.; Moro-oka, Y.; Hashimoto, S.; Kitagawa, T.; Toriumi, K.; Tatsumi, K.; Nakamura, A. *J. Am. Chem. Soc.* **1992**, *114*, 1277–1291.

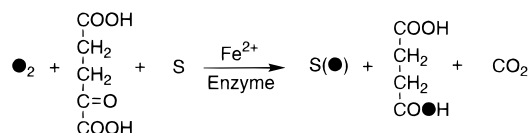
(10) X-ray quality violet needles were obtained over a period of several weeks from an acetone solution at -20°C . **1** crystallizes in the monoclinic space group $P2_1$, with $a = 10.0654(3)$ Å, $b = 21.2126(5)$ Å, $c = 12.0796(3)$ Å, $\beta = 97.307(1)^\circ$, $V = 2558.21(12)$ Å³, and $Z = 2$. The structure was solved and refined with SHELXTL 5.0 (Siemens Industrial Automation: Madison, WI). Two molecules of acetone cocrystallized with each molecule of **1**. 7996 unique reflections were collected to $25.07^\circ 2\theta$ at 173 K with Mo K α ($\lambda = 0.71073$ Å radiation) on a Siemens SMART Platform CCD. The structure was solved by direct methods and refined to $R = 0.0713$ and $R_w = 0.1083$ ($I > 2\sigma(I) = 4890$).

(11) Hikichi, S.; Ogihara, T.; Fujisawa, K.; Kitajima, N.; Akita, M.; Moro-oka, Y. *Inorg. Chem.* **1997**, *36*, 4539–4547.

(12) According to this formalism, a perfect square pyramid would have a τ -value of 0.00, while a perfect trigonal bipyramid would have a τ -value of 1.00 (Addison, A. W.; Rao, T. N.; Reedijk, J.; van Rijn, J.; Verschoor, G. C. *J. Chem. Soc., Dalton Trans.* **1984**, 1349–1356).

(13) In a typical experiment, 1 mg of **1** was dissolved in 1 mL of anaerobic, distilled benzene and then diluted with an additional 2 mL of O_2 -saturated benzene.

Scheme 1



Complex **1** was synthesized by the anaerobic, sequential addition of equimolar amounts of FeCl_2 , $\text{K}(\text{Tp}^{\text{Ph}_2})$,⁹ and the α -keto acid sodium benzoylformate (BF) in an acetonitrile slurry (Supporting Information). The crystal structure of **1**¹⁰ (Figure 1) reveals a 5-coordinate iron(II) center with a monoanionic, face-capping Tp^{Ph_2} and a chelated BF, similar to that of the related complex $[\text{Fe}(\text{Tp}^{\text{Bu}_i\text{-Pr}})(\text{BF})]$;¹¹ two pyrazole nitrogens and a carboxylate oxygen define the equatorial plane of the distorted trigonal bipyramid ($\tau = 0.65$).¹² The optical spectrum of **1** (Figure 2A) exhibits an absorption band at 531 nm ($340 \text{ M}^{-1}\text{cm}^{-1}$) with shoulders at 476 ($210 \text{ M}^{-1}\text{cm}^{-1}$) and 584 nm ($300 \text{ M}^{-1}\text{cm}^{-1}$). This feature, which is diagnostic of an α -keto acid chelated to an iron(II) center through the α -keto and one carboxylate oxygen, is blue-shifted (Figure 2B) when BF is replaced with an aliphatic α -keto acid, pyruvate ($\text{Ph} \rightarrow \text{Me}$), consistent with its assignment to MLCT transitions.^{5,6,11}

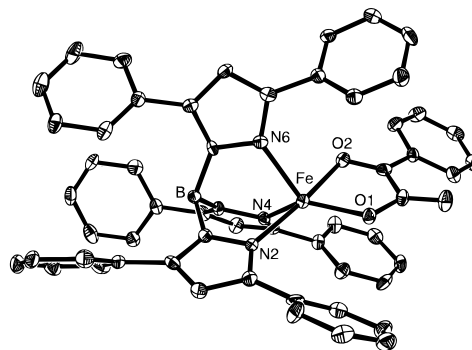


Figure 1. X-ray structure of $[\text{Fe}(\text{Tp}^{\text{Ph}_2})(\text{BF})]$ (**1**) showing 30% probability thermal ellipsoids. Hydrogen atoms and two acetone solvent molecules are omitted for clarity. Selected bond lengths (Å) and distances (deg) are: Fe–O1, 1.968(4); Fe–O2, 2.206(5); Fe–N2, 2.188(5); Fe–N4, 2.068(5); Fe–N6, 2.068(5); O1–Fe–O2, 77.3(2); N2–Fe–N4, 86.4(2); N2–Fe–N6, 89.0(2); N4–Fe–N6, 91.1(2); O1–Fe–N2, 110.1(2); O2–Fe–N2, 171.7(2); O1–Fe–N4, 132.6(2); O2–Fe–N4, 85.7(2); O1–Fe–N6, 131.5(2); O2–Fe–N6, 88.5(2).

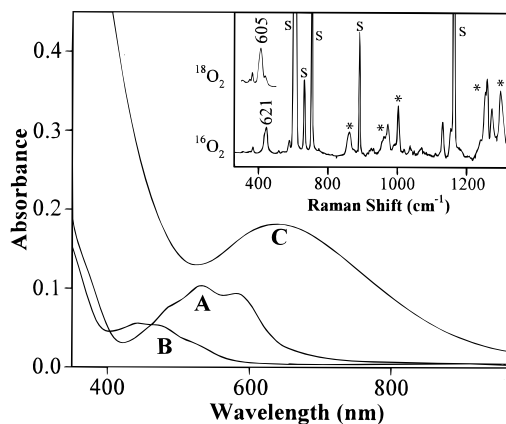
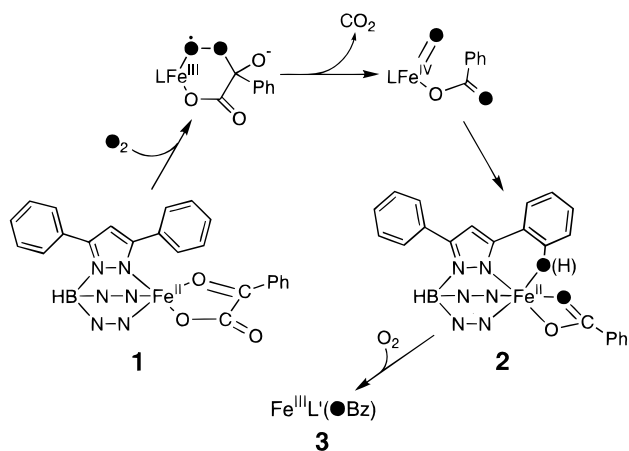


Figure 2. Optical spectra of (A) a 0.25 mM solution of **1** ($R = \text{Ph}$), (B) a 0.25 mM solution of the corresponding pyruvate complex ($R = \text{Me}$), and (C) the product **3** formed from the reaction of 0.25 mM **1** with excess O_2 . Inset: resonance Raman spectra of **3** obtained from frozen CH_2Cl_2 solutions with 632.8 nm excitation.

Scheme 2



Complex **1** reacts with O_2 over the course of 30 min¹³ affording the quantitative decarboxylation of BF to benzoic acid.¹⁴ Concomitant with this transformation is the generation of a green species (**3**) ($\lambda_{max} = 650$ nm, Figure 2C) whose resonance Raman spectrum (Figure 2 inset) exhibits features characteristic of an iron(III) coordinated to an ortho-substituted phenolate.¹⁵ The identical product is also obtained when $[Fe(Tp^{Ph_2})(OBz)]$ is exposed to O_2 , but the reaction takes approximately 14 h. The analogous green species generated from the reaction of O_2 with $[Fe(Tp^{Ph,Me})(OOCR)]$ has been identified by Fujisawa et al. to be an iron(III) complex in which one of the 3-phenyl groups of the Tp ligand is hydroxylated.¹⁶ Combined, these results demonstrate that **1** reacts with O_2 to form **2**, which autoxidizes to green **3** (Scheme 2).

The fate of dioxygen was established by $^{18}O_2$ -labeling experiments (95%, Cambridge Isotope). Analysis of the OBz product via GC-mass spectrometry demonstrated that approximately 80% of the newly formed carboxylate contained one atom of oxygen from O_2 . The substoichiometric incorporation is consistent with previously published results and is attributed to a competing autoxidation reaction.⁶ The other ^{18}O atom is incorporated into the phenolate product as evidenced by the diagnostic shifts in key peak frequencies in the resonance Raman spectrum.^{17,18} Incorporation of the label into the phenolate is nearly quantitative (90%) as deduced from the intensity of the residual 621 cm^{-1} peak ($\nu_{Fe-16OAr}$) relative to that of the 605 cm^{-1} peak ($\nu_{Fe-18OAr}$) (Figure 2 inset). Thus, **1** reproduces the dioxygenase nature of

(14) Benzoate was formed stoichiometrically as determined via GC. Quantification entailed decomposing the inorganic complex with 0.1 M H_2SO_4 , extracting the organic products with Et_2O and $CHCl_3$, and esterifying with diazomethane according to standard procedures. Methyl 3-chlorobenzoate was added after degradation of the complex as an internal standard.

(15) Carrano, C. J.; Carrano, M. W.; Sharma, K.; Backes, G.; Sanders-Loehr, J. *Inorg. Chem.* **1990**, *29*, 1865–1870.

(16) Fujisawa, K.; Suezaki, M.; Moro-oka, Y., submitted for publication.

(17) Raman frequencies (cm^{-1}) of dioxygen-sensitive peaks of sample prepared with $^{16}O_2$ or ($^{18}O_2$): 621 (605); 861 (844); 961 (942); 1254 (1245); and 1298 (1294).

(18) Pyrz, J. W.; Roe, A. L.; Stern, L. J.; Que, L., Jr. *J. Am. Chem. Soc.* **1985**, *107*, 614–620.

(19) Lindblad, B.; Lindstedt, G.; Lindstedt, S. *J. Am. Chem. Soc.* **1970**, *92*, 7446–7449.

(20) These complexes were synthesized in a manner analogous to that of **1** except that $Fe(ClO_4)_2$ was utilized in place of $FeCl_2$ and the reaction was performed in MeOH. The insoluble products were collected by filtration.

(21) Kim, K.; Lippard, S. J. *J. Am. Chem. Soc.* **1996**, *118*, 4914–4915.

(22) Kitajima, N.; Tamura, N.; Amagai, H.; Fukui, H.; Moro-oka, Y.; Mizutani, Y.; Kitagawa, T.; Mathur, R.; Heerwegh, K.; Reed, C. A.; Randall, C. R.; Que, L., Jr.; Tatsumi, K. *J. Am. Chem. Soc.* **1994**, *116*, 9071–9085.

(23) Sono, M.; Roach, M. P.; Coulter, E. D.; Dawson, J. H. *Chem. Rev.* **1996**, *96*, 2841–2887.

(24) Wallar, B. J.; Lipscomb, J. D. *Chem. Rev.* **1996**, *96*, 2625–2657.

α -keto acid-dependent enzymes (Scheme 1) and, in particular, mimics *p*-hydroxyphenylpyruvate dioxygenase in its ability to hydroxylate a phenyl ring.¹⁹

Steric effects play a key role in modulating the reactivity of α -keto acid complexes. Whereas **1** reacts with O_2 within 30 min, the sterically encumbered $[Fe(Tp^{i-Bu,i-Pr})(BF)]$ is completely unreactive toward O_2 .¹¹ Consistent with this trend, $[Fe(Tp^{Me_2})(BF)]$ reacts with O_2 within minutes.⁷ Furthermore, when the phenyl group of the BF moiety on **1** is replaced with Me or *i*-Pr,²⁰ the resulting complexes effect arene hydroxylation significantly faster. The order of reactivity for the different R groups is $Ph < i-Pr < Me$, with R = Me reacting almost an order of magnitude faster than BF. This is the opposite of what is expected based on previous results where electron-withdrawing groups on ring-substituted BFs enhanced reactivity, which was consistent with a partially rate-limiting nucleophilic attack of an Fe-bound superoxide on the α -carbon.⁶ Taken together, these results indicate that steric constraints are an important determinant of the reactivity and suggest that the transformation of the O_2 adducts into products entails molecular motions that require ample space around the iron center.

The fact that both **1** and $[Fe(Tp^{Ph_2})(OBz)]$ react with O_2 to produce **3** suggests that these complexes generate related, if not identical, oxidizing agents during the course of the reaction. An attractive intermediate is a $[(Tp^{Ph_2})Fe^{IV}=O]$ species. The 30-fold difference in reactivity between these two complexes (0.5 h vs 14 h) thus can be rationalized by the differing mechanisms each utilizes to form the putative oxene species. $[Fe(Tp^{Ph_2})(OBz)]$ very likely generates the iron-oxo species via O–O bond lysis of a (μ -1,2-peroxo)diiron(III) intermediate, which has previously been observed and crystallized for a Tp^{i-Pr_2} derivative.^{21,22} Complex **1**, on the other hand, is proposed to form the iron-oxo species via lysis of a mononuclear iron-peroxo species, derived from nucleophilic attack of the Fe^{III} -bound superoxide onto the α -carbon of the keto acid (Scheme 2).⁶ Significantly, the activation energy for O–O bond cleavage may be lowered considerably by coupling this step to the loss of CO_2 . Thus, **1** effects arene hydroxylation significantly faster than $[Fe(Tp^{Ph_2})(OBz)]$, highlighting the importance of the α -keto acid in activating O_2 .

In conclusion, $[Fe(Tp^{Ph_2})(BF)]$ is both a structural and functional mimic of α -keto acid-dependent enzymes. The mono-anionic, tridentate, facially capping Tp^{Ph_2} ligand approximates the endogenous 2-His-1-carboxylate facial triad found in DAOCS, BF chelates to the iron center, and an available coordination site is maintained for binding O_2 . Upon exposure of **1** to O_2 , BF undergoes oxidative decarboxylation, and the Tp^{Ph_2} ligand is hydroxylated, with 1 atom of oxygen being incorporated into each product, mimicking for the first time the dioxygenase nature of the enzymatic reaction. The use of the α -keto acid cofactor thus allows these enzymes to activate dioxygen and generate a versatile oxidant via a mechanism which is distinct from those of enzymes that require a porphyrin ring²³ or a second metal ion.²⁴

Acknowledgment. The authors thank Professor Kiyoshi Fujisawa (Tokyo Institute of Technology) for sharing unpublished results and Dr. Victor G. Young, Jr. (University of Minnesota) for solving the crystal structure of **1**. This work has been supported by the National Institutes of Health (GM33162), and NIH postdoctoral fellowship support for E.L.H. (GM18639) and R.Y.N.H. (GM17849) is gratefully acknowledged.

Supporting Information Available: Further experimental details concerning the synthesis and characterization of **1**, $[Fe(Tp^{Ph_2})(pyruvate)]$, $[Fe(Tp^{Ph_2})(O_2CC(O)CH(CH_3)_2)]$, and $[Fe(Tp^{Ph_2})(OBz)]$, full resonance Raman spectra of **3**, and tables of crystal data, data collection, structure solution and refinement, atomic coordinates, and bond lengths and angles for **1** are available (PDF). This material is available free of charge via the Internet at <http://pubs.acs.org>.

JA983867U